

Articles

Fabrication of Diameter-tunable Well-aligned ZnO Nanorod Arrays via a Sonochemical Route

Seung-Ho Jung, Eugene Oh,[†] Kun-Hong Lee,^{*} Soo-Hwan Jeong,^{†,*} Yosep Yang,[‡] and Chan Gyung Park[‡]

Department of Chemical Engineering, Pohang University of Science and Technology, Pohang 790-784, Korea
^{*}E-mail: ce20047@postech.ac.kr

[†]Department of Chemical Engineering, Kyungpook National University, Daegu 702-701, Korea. ^{*}E-mail: shjeong@knu.ac.kr

[‡]Department of Material Science and Engineering, Pohang University of Science and Technology, Pohang 790-784, Korea
Received April 19, 2007

A simple and facile sonochemical route was described for the fabrication of diameter-controlled ZnO nanorod arrays on Si wafers. The diameter of ZnO nanorods was controlled by the concentration of zinc cations and hydroxyl anions in aqueous precursor solution. At high concentration of the precursor solution, thick ZnO nanorod arrays were formed. On the contrary, thin ZnO nanorod arrays were formed at low concentration of the precursor solution. The average diameter of ZnO nanorods varies from 40 to 200 nm. ZnO nanorod arrays with sharp tip were also fabricated by the step-by-step decrease in precursor solution concentration. The crystal structure and optical characteristics of ZnO nanorods were investigated by transmission electron microscopy, X-ray diffraction, and photoluminescence spectroscopy. Growth mechanism of ZnO nanorod arrays was also proposed.

Key Words : Zinc oxide, Nanorod, Diameter control, Ultrasound

Introduction

One-dimensional (1D) semiconductor nanostructures have attracted considerable attention for potential applications, such as nanoelectronics and optoelectronics, due to their unusual properties based on nanometer-scale dimension. Zinc oxide (ZnO) is one of the most important multi-functional semiconductors with its wide direct energy band gap of 3.37 eV and its large exciton binding energy (about 60 meV). Thus, 1D ZnO nanostructures has been the topic of intensive investigation in the field of nanolasers,¹ electrodes for solar cells,² field emitters,³ field-effect transistors,⁴ and so on. In particular, after the report of room temperature ultraviolet lasing in ZnO nanowire arrays,¹ well-aligned 1D ZnO nanostructures with tunable diameters have been very useful research tools to investigate the size effect on physical properties of 1D semiconductor nanostructures. To date, various approaches related to direct growth of diameter-controlled ZnO nanorod or nanowire arrays on substrates were reported, and the development of new synthetic methodologies is still ongoing.

Conventional approaches for controlling the diameter of well-aligned 1D ZnO nanostructures have been based on vapor-phase reaction.⁵⁻⁷ By adjusting the growth conditions, including reaction temperature, oxygen-to-zinc flux ratio, and size of metal catalysts, vapor-phase methods can produce highly-crystalline and well-aligned 1D ZnO nanostructures with different diameters, however, they require sophisticated equipments due to rigorous environmental

conditions, such as high temperature (up to 1400 °C) and low pressure. Such severe environmental conditions are inadequate for nanoelectronic circuit integration in glass-based transparent electrode devices or polymer-based flexible devices. In addition to the conventional vapor-phase methods, solution-phase methods have been developed as alternative ways. Among all solution-based approach, a hydrothermal method^{8,9} is a widely-used technique that can produce well-aligned and diameter-tuned 1D ZnO nanostructures by adjusting the growth conditions, such as reaction temperature, concentration of precursor solution, pH, and reaction time. Unlike the conventional vapor-based approaches, a hydrothermal method is a relatively low temperature (below 200 °C) process and requires simple equipments, however, long reaction time (usually from a few hours to several days) is the weak point of this method. Therefore the development of a simple and fast synthetic route which can control the diameter of well-aligned 1D ZnO nanostructures under ambient conditions remained an important topic of investigation.

By the use of chemical effects of ultrasound, a sonochemical method has been recently investigated as a promising alternative technique for the fabrication of colloidal ZnO nanorods under ambient conditions.^{10,11} Cavitation phenomena play a key role in the sonochemical synthesis of ZnO nanorods. Cavitation is the formation of microbubbles in a liquid when a large negative pressure is applied to the liquid by the transmission of ultrasound. Large amount of energy, temperatures of 5000 K and pressures of up to 1800

atmospheres,¹²⁻¹⁴ is known to be released from the collapse of microbubbles during ultrasonic cavitation. However, due to the extremely high cooling rates in excess of 10^{10} K/s by the surrounding bulk liquid,^{15,16} sonochemical synthesis of ZnO nanorods is possible under normal temperature and pressure without additional heating the solution. So, this sonochemical approach is fast, simple, convenient, economical, and environmentally benign. Very recently, we reported sonochemical growth of well-aligned ZnO nanorod arrays on various substrates over large areas.¹⁷ Herein, we report the diameter control of well-aligned ZnO nanorod arrays *via* a sonochemical route. We also show the morphology control of ZnO nanorod tips.

Experimental Section

All chemical reagents were used without further purification. Before the growth of ZnO nanorod arrays, Ti (5 nm for adhesion layer) and Zn (40 nm for seed layer) thin films were sputtered successively on $3\text{ cm} \times 3\text{ cm}$ Si wafers. Then, four thin films-coated Si wafers were immersed in 0.001, 0.01, 0.05, and 0.1 M equimolar aqueous solutions of zinc nitrate hexahydrate ($\text{Zn}(\text{NO}_3)_2 \cdot 6\text{H}_2\text{O}$, 98%, Aldrich) and hexamethylenetetramine (HMT, $(\text{CH}_2)_6\text{N}_4$, 99%, Junsei), respectively. Ultrasonication was performed by sonochemical apparatus (ultrasonic frequency of 20 kHz) under ambient conditions in order to grow diameter-tunable well-aligned ZnO nanorod arrays. An ultrasonic wave was introduced at the power of 50 W (intensity of 39.5 W/cm^2) for 1 h by 1/2 inch diameter titanium tip. Except for the difference in equimolar concentration of precursor solutions which contain zinc nitrate hexahydrate and HMT, four samples were prepared under the same ultrasonication power and reaction time. The ZnO-grown Si wafers were carefully washed with de-ionized (DI) water, and then dried in an oven.

For the growth of ZnO nanorod arrays with sharp tips, Ti (5 nm) and Zn (40 nm) thin films-coated Si wafer was immersed in a 0.1 M equimolar aqueous solutions of zinc nitrate hexahydrate and HMT. The ultrasonic wave was introduced at the intensity of 39.5 W/cm^2 for 30 min. Then, the process was repeated twice in a 0.01 M and a 0.001 M equimolar aqueous solutions step-by-step using the previous ZnO-grown Si wafer. Ultrasonication intensities and reaction times were fixed at 39.5 W/cm^2 and 30 min, respectively. The ZnO-grown Si wafer was carefully washed with DI water, and then dried in an oven.

The morphology of the ZnO nanorod arrays was observed by field emission scanning electron microscope (FESEM, Hitachi S-4300). The crystallinity and crystal structures were investigated by transmission electron microscope (TEM, JEOL JEM-2010). The orientation and alignment were examined by X-ray diffraction (XRD, Max Science, M18XHF). Room-temperature photoluminescence (PL) characteristics of ZnO nanorod arrays, which have shown different diameters, were investigated by using PL spectroscopy (Shimadzu RF-5301PC). The PL spectra were excited

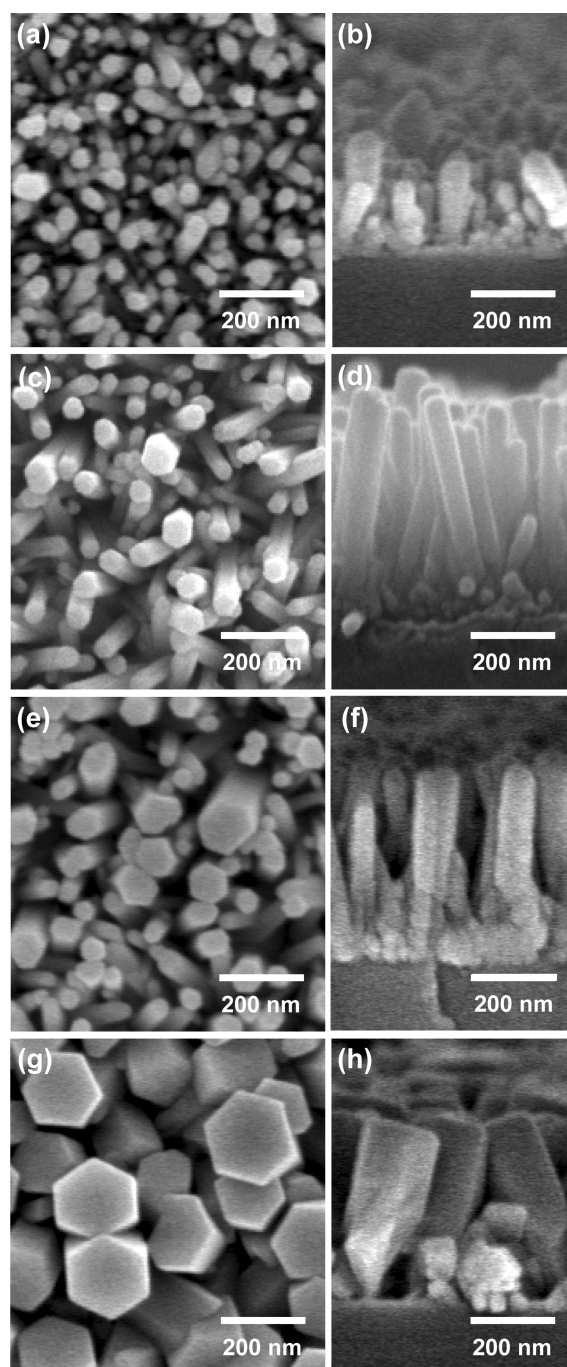


Figure 1. (a), (c), (e), and (g) Top view SEM images of ZnO nanorod arrays grown on Si wafers at 0.001, 0.01, 0.05, and 0.1 M equimolar aqueous solutions of zinc nitrate hexahydrate and HMT, respectively. (b), (d), (f), and (h) Side view SEM images of ZnO nanorod arrays grown on Si wafers at 0.001, 0.01, 0.05, and 0.1 M precursor solutions, respectively.

by a 150 W Xe lamp and detected by a photomultiplier after dispersed by a concave grating.

Results and Discussion

Figure 1 shows FESEM images of ZnO nanorod arrays with different diameters on Si wafers. Hexagon-shaped dia-

meter-tunable ZnO nanorod arrays were vertically well-aligned throughout the surface of Si wafer. The average diameter increased from 46 to 198 nm as the concentration of precursor solution increased from 0.001 to 0.1 M, as shown in Figures 1. The increase in the concentration of precursor solution means the increase in the amount of both zinc cations (Zn^{2+} ions) and hydroxyl anions (OH^- ions) which react with each other in order to form stable $\text{Zn}(\text{OH})_4^{2-}$ complexes, growth units of ZnO nanorods. During the crystallization of ZnO, OH^- ions contained at the surface of ZnO crystal have a shielding effect on the growth of ZnO nanorods.¹⁸ Due to the increase of shielding effect of OH^- ions at the interface of the (0001) face, as the concentration of precursor solution increases from 0.01 M, the growth rate of the (0001) face is thought to decrease greatly relative to other crystal faces. Therefore we expect that increase in the amount of growth units of ZnO cause the increase in diameters of ZnO nanorods due to the radial growth along the $\langle 01\text{-}10 \rangle$ direction. It is noted that average diameter of ZnO nanorods proportionally increased according to the increase in the concentration of precursor solution. At too high concentration of 0.1 M, slight overlap between adjacent ZnO nanorods was also observed (Figure 1g).

From side view SEM images, we also observed that the average lengths of ZnO nanorods were affected by the concentration of precursors. From Figure 1b and d, lengths of ZnO nanorods increased as the concentration of precursor solution increased from 0.001 to 0.01 M under the same ultrasonication time. It is thought that this is due to the increase in the amount of growth units of ZnO nanostructures. However, as the concentration of precursor solution increased from 0.01 to 0.1 M, the average length of ZnO nanorods decreased under the same ultrasonication time (Figure 1d, f and h). As the concentration of precursor solution increases, the amount of NH_4^+ ions produced from the hydration of HMT also increases. Therefore, $\text{Zn}(\text{OH})_{4-x}(\text{ONH}_4)_x^{2-}$ complexes are thought to be formed as the NH_4^+ ions become to bond with $\text{Zn}(\text{OH})_4^{2-}$, and these $\text{Zn}(\text{OH})_{4-x}(\text{ONH}_4)_x^{2-}$ complexes should be converted to $\text{Zn}(\text{OH})_4^{2-}$ before ZnO crystals growth. The conversion reaction tends to be an endothermic process, which hinders the growth of ZnO nanorods. Thus, due to the endothermic conversion reaction and the larger shielding effect of OH^- ions at the interface of the (0001) face, the average length of ZnO nanorods was shortened as the concentration of precursor solution increases over 0.01 M.¹⁸ Below the concentration of 0.01 M, it seems that endothermic conversion reaction and shielding effect of OH^- ions are not critical. Unlike the proportional trend in diameters of ZnO nanorods with regard to the concentration of precursor solution, average length is out of proportion.

As mentioned above, we observed concentration effect of precursors on average length of ZnO nanorods as the concentration of precursor solution increased. Although there is the difference between the average lengths of ZnO nanorods grown at four different concentration solutions, this difference in average length can be controlled by only

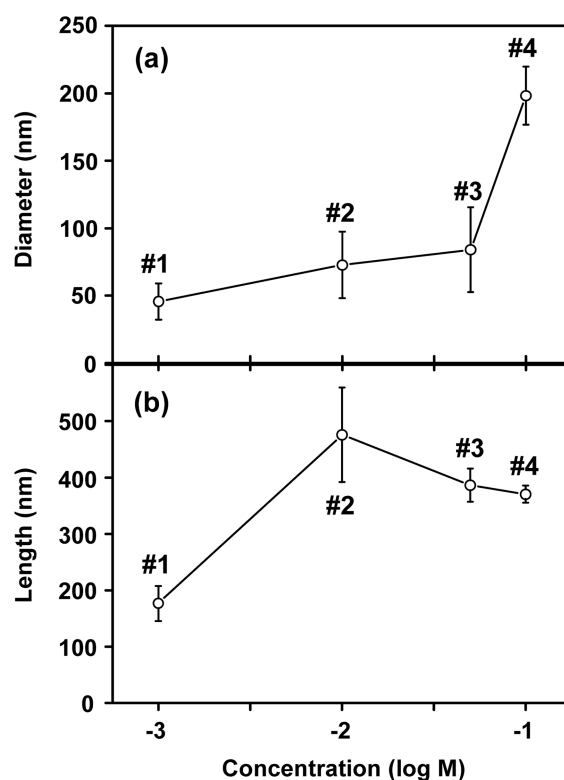
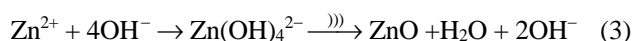
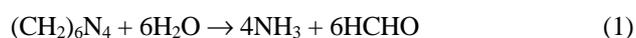


Figure 2. Changes in (a) diameter and (b) length of ZnO nanorod arrays as a function of the equimolar concentration of zinc nitrate hexahydrate and HMT in aqueous solution. Open circles represent average diameters and lengths of ZnO nanorod arrays, and standard deviation is shown as error bars. Samples 1-4 represent the ZnO nanorod arrays grown on Si wafers at 0.001, 0.01, 0.05, and 0.1 M precursor solutions, respectively.

varying the ultrasonication time. We already showed that the length of ZnO nanorod arrays can be controlled by ultrasonication time in our previous report.¹⁷

Figure 2 summarized above concentration dependency of diameters and lengths of ZnO nanorod arrays. In this paper, samples 1-4 represent the ZnO nanorod arrays grown on Si wafers at 0.001, 0.01, 0.05, and 0.1 M precursor solutions, respectively. As shown in Figure 2a and b, samples 1-4 showed average diameters of 46, 73, 84, and 198 nm, and average lengths of 177, 476, 386, and 370 nm, respectively. From Figure 1 and 2, ZnO nanorod arrays with different diameters could be successfully synthesized under the current sonochemical route by adjusting equimolar concentration of zinc nitrate hexahydrate and HMT in aqueous solution.

The growth mechanism of ZnO nanorod arrays on Si wafer was considered as follows:^{11,17,18}



where the symbol))) denotes ultrasonic irradiation.

In general, radicals, such as $\cdot\text{H}$, $\cdot\text{OH}$, $\cdot\text{O}_2^-$ and $\cdot\text{HO}_2$, are

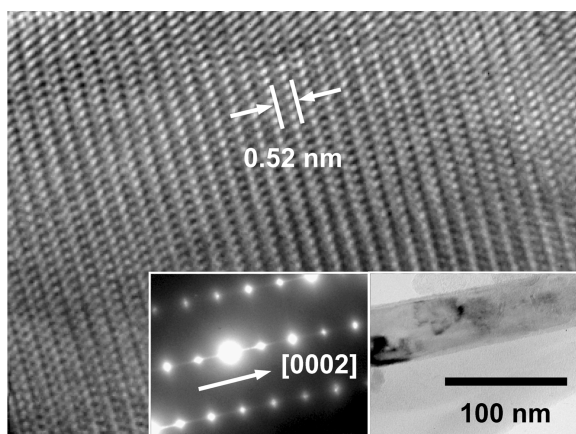
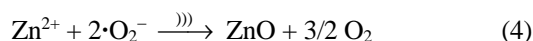


Figure 3. A HRTEM image of a single ZnO nanorod produced at a 0.01 M equimolar aqueous solution of zinc nitrate hexahydrate and HMT. Two insets are an electron diffraction pattern (the left inset) and a low magnification TEM image (the right inset).

generated in the sonolysis of water under the air atmosphere.¹⁹⁻²¹ Among them, $\cdot\text{O}_2^-$ radicals are known to participate in the growth of ZnO nanorods.²² Therefore, ZnO nanorods also can be grown by the next reaction path:



In the initial growth stage of the ZnO nanorods, the Zn thin film, which was deposited onto a Si wafer, mainly acts as nucleation sites. When Zn thin film is used as a seed layer, uniform growth and in-plane alignment of ZnO nanorod arrays are improved. Zn^{2+} and OH^- ions for ZnO growth on a Si wafer were supplied from hydration process of zinc nitrate hexahydrate and HMT, respectively. The concentration of zinc nitrate hexahydrate and HMT affects both the diameters and the lengths of ZnO nanorod arrays as mentioned above. ZnO nanorods grow preferentially along the [0001] direction due to the higher growth rate along the [0001] direction.¹⁸ Considering the high density of our samples (about $10^{10}/\text{cm}^2$), steric hindrance effect^{23,24} is also expected to contribute the vertical alignment of ZnO nanorod arrays.

ZnO nanorods were separated from the Si wafers for crystal structure analysis. Figure 3 shows a HRTEM image of a single ZnO nanorod detached from the sample 2. Two insets in Figure 3 are an electron diffraction pattern (the left inset) and a low magnification TEM image (the right inset). From the HRTEM image, ZnO nanorods are highly-crystalline with a lattice spacing of about 0.52 nm which corresponds to the d -spacing of (0001) planes in hexagonal ZnO crystal lattice. With the TEM observation, the electron diffraction pattern suggests that ZnO nanorods grew along the [0001] direction, polar c -axis of the ZnO crystal lattice. ZnO nanorods, which were separated from other samples (sample 1, 3, and 4), showed the same results as mentioned above.

This is consistent with the results of the XRD patterns. Figure 4 shows the XRD patterns of ZnO nanorod arrays

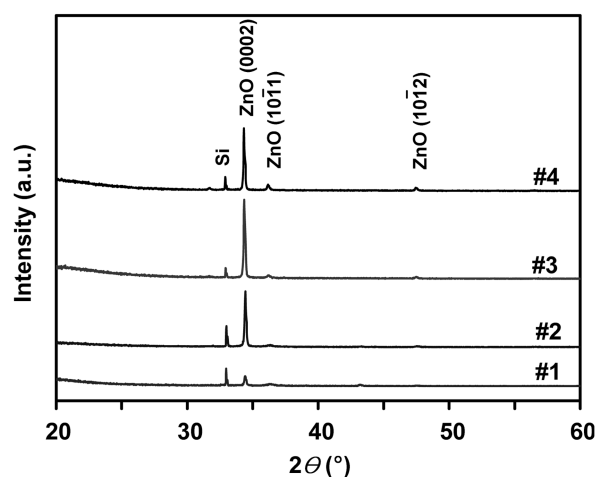


Figure 4. XRD patterns of ZnO nanorod arrays with different diameters on Si wafer. Samples 1-4 represent the ZnO nanorod arrays grown on Si wafers at 0.001, 0.01, 0.05, and 0.1 M precursor solutions, respectively. A diffraction peak related to Si is due to Si $\langle 100 \rangle$ wafer.

with different diameters on Si wafers. The XRD pattern of sample 1 shows a small peak at about 34° due to ZnO (0002) planes with a large peak at about 33° due to Si $\langle 100 \rangle$ wafer. Short ZnO nanorod arrays are thought to be the reason for the small peak intensity at about 34° . The XRD patterns of samples 2-4 show very sharp peaks at about 34° due to ZnO (0002) planes with small peaks at about 33° due to Si wafer. Although diffraction peaks due to ZnO (10-11) and (10-12) planes were shown in XRD patterns of samples 1-4, intensities of both peaks were very small with respect to that of a diffraction peak due to ZnO (0002) planes. This means that ZnO nanorods with different diameters were vertically well-aligned on Si wafers along [0001] direction. Pure hexagonal-phase ZnO nanorod arrays were synthesized under the current sonochemical method. This was because there was

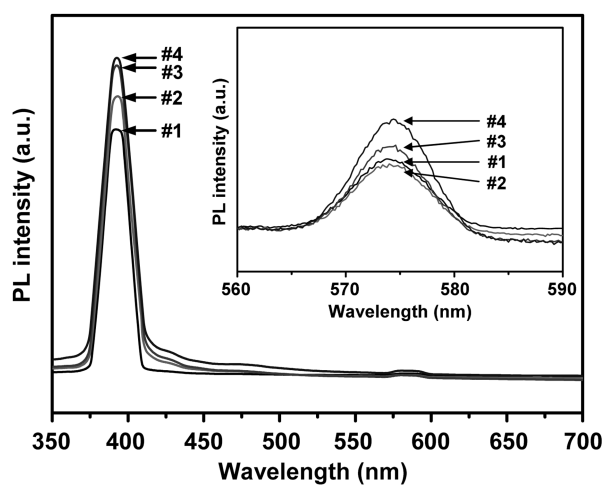


Figure 5. Room temperature PL spectra of ZnO nanorod arrays with different diameters on Si wafer. Samples 1-4 represent the ZnO nanorod arrays grown on Si wafers at 0.001, 0.01, 0.05, and 0.1 M precursor solutions, respectively. The inset shows weak deep level emissions in visible range.

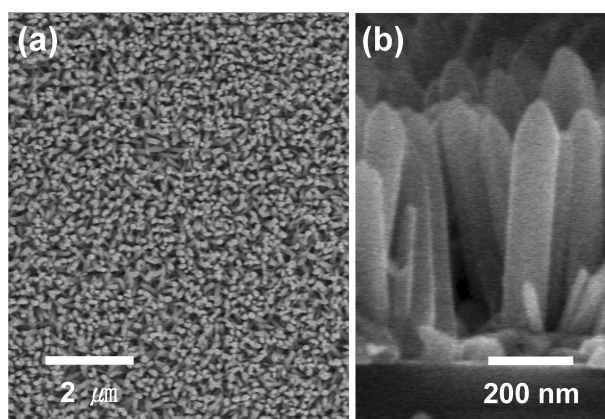


Figure 6. SEM images of ZnO nanorod arrays with sharp tips. (a) A top view SEM image of low magnification. (b) A side view SEM image of high magnification.

no diffraction peaks observed from other impurities in the XRD patterns. From TEM and XRD pattern analyses, we confirmed that highly crystalline ZnO nanorod arrays, with different diameters, were vertically well-aligned on the substrates along [0001] direction.

PL measurements were conducted at room temperature to investigate the optical property of diameter-tunable ZnO nanorod arrays on a Si wafer as shown in Figure 5. Samples 1-4 show the similar PL features, dominant UV emission (at about 390 nm, which corresponds to about 3.18 eV) with negligible deep level emission. When we examined the deep level emission in detail, samples 1-4 showed the green-yellow emission (from 570 nm to 580 nm in the inset of Fig. 5) due to oxygen vacancies.^{6,25} While the intensities of green-yellow emission of samples 1-3 are similar each other, the intensity of green-yellow emission of sample 4 is slightly larger than those of samples 1-3. PL intensity is a function of excitation laser intensity, ZnO nanorods film temperature, and interface quality. We believe that slight difference in visible PL emission intensities of four samples is due to the excitation laser intensity rather than the level of structural defects. The typical laser varies by 10-20% at times. Considering the negligible intensities of deep level emission relative to UV emission, all samples prepared by our sonochemical method have high optical quality.

In addition to the fabrication of diameter-tunable ZnO nanorod arrays, the sonochemical growth of well-aligned ZnO nanorod arrays with sharp tips was successfully conducted on a Si wafer as shown in Figure 6. The average diameter of bottom part and entire length were 98 and 616 nm, respectively. Evolution of ZnO nanorods into nano-needles due to the step-by-step decrease in the amount of Zn vapor source was previously reported.²⁶ It is believed that ZnO nanorods with sharp tips were formed by the step-by-step decrease in the concentration of precursor solution from 0.1 to 0.001 M. Decrease in the concentration level of precursor solution results in the decrease in the amount of ZnO growth units. Direct growth of aligned ZnO nanorods with sharp tips is highly desirable for the design of high-performance nanodevices, such as field emitter arrays.

Conclusion

The sonochemical growth of diameter-tunable well-aligned ZnO nanorod arrays on the substrate with high density was demonstrated. This sonochemical technique is fast, simple, convenient, economical, and environmentally benign. Concentration level of Zn^{2+} and OH^- ions in aqueous precursor solution was a key factor in the fabrication of ZnO nanorod arrays with different diameters. FESEM showed that the average diameter was controlled from 46 to 198 nm as the concentration of precursor solution changed from 0.001 to 0.1 M. TEM and XRD revealed the preferential c-axis oriented growth of highly crystalline ZnO nanorod arrays on the substrate. The well-aligned ZnO nanorod arrays showed outstanding optical characteristics, that is, dominant UV emission at about 390 nm which corresponds to about 3.18 eV with negligible green-yellow emission. With some modifications, we also demonstrated the sonochemical growth of ZnO nanorod arrays with sharp tips. We expect that this sonochemical technique can be very useful in seeking to design high-performance ZnO-based nanodevices.

Acknowledgment. This work was supported by the Tera-level Nanodevices (TND) Program of the Korean Ministry of Science and Technology.

References

- Huang, M. H.; Mao, S.; Feick, H.; Yan, H.; Wu, Y.; Kind, H.; Weber, E.; Russo, R.; Yang, P. *Science* **2001**, *292*, 1897.
- Kim, K. S.; Kang, Y.-S.; Lee, J.-H.; Shin, Y.-J.; Park, N.-G.; Ryu, K. S.; Chang, S. H. *Bull. Korean Chem. Soc.* **2006**, *27*, 295.
- Zhu, Y. W.; Zhang, H. Z.; Sun, X. C.; Feng, S. Q.; Xu, J.; Zhao, Q.; Xiang, B.; Wang, R. M.; Yu, D. P. *Appl. Phys. Lett.* **2003**, *83*, 144.
- Ng, H. T.; Han, J.; Yamada, T.; Naguyen, P.; Chen, Y. P.; Meyyappan, M. *Nano Lett.* **2004**, *4*, 1247.
- Cong, G. W.; Wei, H. Y.; Zhang, P. F.; Peng, W. Q.; Wu, J. J.; Liu, X. L.; Jiao, C. M.; Hu, W. G.; Zhu, Q. S.; Wang, Z. G. *Appl. Phys. Lett.* **2005**, *87*, 231903.
- Yang, P.; Yan, H.; Mao, S.; Russo, R.; Johnson, J.; Saykally, R.; Morris, N.; Pham, J.; He, R.; Choi, H.-J. *Adv. Funct. Mater.* **2002**, *12*, 323.
- Wu, J.-J.; Liu, S.-C. *J. Phys. Chem. B* **2002**, *106*, 9546.
- Guo, M.; Diao, P.; Cai, S. *J. Solid State Chem.* **2005**, *178*, 1864.
- Zhang, Z.; Yu, H.; Shao, X.; Han, M. *Chem. Eur. J.* **2005**, *11*, 3149.
- Zhang, X.; Zhao, H.; Tao, X.; Zhao, Y.; Zhang, Z. *Mater. Lett.* **2005**, *59*, 1745.
- Hu, X. L.; Zhu, Y. J.; Wang, S. W. *Mater. Chem. Phys.* **2004**, *88*, 421.
- Suslick, K. S.; Price, G. J. *J. Ann. Rev. Mater. Sci.* **1999**, *29*, 295.
- Suslick, K. S.; Hammerton, D. A.; Cline, Jr., R. E. *J. Am. Chem. Soc.* **1986**, *108*, 5641.
- Pol, V. G.; Reisfeld, R.; Gedanken, A. *Chem. Mater.* **2002**, *14*, 3920.
- Suslick, K. S. *Science* **1990**, *247*, 1439.
- Flint, E. B.; Suslick, K. S. *Science* **1991**, *253*, 1397.
- Jung, S.-H.; Oh, E.; Lee, K.-H.; Park, W.; Jeong, S.-H. *Adv. Mater.* **2007**, *19*, 749.
- Li, W. J.; Shi, E. W.; Zhong, W. Z.; Yin, Z. W. *J. Cryst. Growth* **1999**, *203*, 186.

19. Destailats, H.; Lesko, T. M.; Knowlton, M.; Wallace, H.; Hoffmann, M. R. *Ind. Eng. Chem. Res.* **2001**, *40*, 3855.
 20. Mason, T. J. *Sonochemistry*; Oxford University Press: New York, 1999; p 16.
 21. Destailats, H.; Colussi, A. J.; Joseph, J. M.; Hoffmann, M. R. *J. Phys. Chem. A* **2000**, *104*, 8930.
 22. Chaparro, A. M.; Maffiotte, C.; Gutiérrez, M. T.; Herrero, J. *Thin Solid Films* **2003**, *431-432*, 373.
 23. Ren, Z. F.; Huang, Z. P.; Xu, J. W.; Wang, J. H.; Bush, P.; Siegal, M. P.; Provencio, P. N. *Science* **1998**, *282*, 1105.
 24. Lee, C. J.; Kim, D. W.; Lee, T. J.; Choi, Y. C.; Park, Y. S.; Lee, Y. H.; Choi, W. B.; Lee, N. S.; Park, G.-S.; Kim, J. M. *Chem. Phys. Lett.* **1999**, *312*, 461.
 25. Vanheusden, K.; Warren, W. L.; Seager, C. H.; Tallant, D. R.; Voigt, J. A.; Gnade, B. E. *J. Appl. Phys.* **1996**, *79*, 7983.
 26. Zhang, Z.; Yuan, H.; Zhou, J.; Liu, D.; Luo, S.; Miao, Y.; Gao, Y.; Wang, J.; Liu, L.; Song, L.; Xiang, Y.; Zhao, X.; Zhou, W.; Xie, S. *J. Phys. Chem. B* **2006**, *110*, 8566.
-